Available online at www.sciencedirect.com

ScienceDirect

Acta Materialia 91 (2015) 255–266

Acta MATERIALIA

www.elsevier.com/locate/actamat

Strain hardening and dislocation avalanches in micrometer-sized dimensions

Jorge Alcalá,[a,*] Jan Očenášek,[b] Kai Nowag,[c] Daniel Esqué-de los Ojos,[c] Rudy Ghisleni[c] and Johann Michler[c]

[a]*Department of Materials Science and Metallurgical Engineering, GRICCA, EUETIB and ETSEIB, Universitat Politècnica de Catalunya, 08028 Barcelona, Spain*

[b]*New Technologies Research Centre, University of West Bohemia in Pilsen, 30614 Plzeň, Czech Republic*

[c]*Laboratory for Mechanics of Materials and Nanostructures, EMPA – Swiss Federal Laboratories for Materials Science and Technology, 3602 Thun, Switzerland*

Received 1 September 2014; revised 13 February 2015; accepted 13 February 2015
Available online 31 March 2015

Abstract—Present experiments and computational simulations furnish a fundamental background to the understanding of plastic flow across sample sizes. It is shown that self-organized criticality (SOC) governs the size distribution of dislocation avalanches in micrometer-sized sample dimensions. Onset of SOC denotes inception of a dislocation network so that dislocation avalanches occur at constant criticality level irrespectively of the applied stress. In these microcrystals, we find that the ratio between the characteristic sample dimension and the mean free path traveled by the mobile dislocations, D/L_{eff}, rules the onset of strain hardening. This index simultaneously accounts for the role of loading orientation and dislocation density upon microscale plasticity. It is shown that strain-hardening emerges for $D/L_{eff} > 2$, where surface dislocation annihilations are inconsequential to network development and the flow stress scales with dislocation density. This regime naturally evolves toward bulk plasticity at increasing sample sizes. Conversely, strain hardening is suppressed when confining sample dimensions dominate plastic flow for $D/L_{eff} < 1.5$. Confining microscale plasticity is characterized by a significant increase in the size of dislocation avalanches under a stagnant dislocation network.

Keywords: Crystal plasticity; Mechanical properties; Dislocations; Strain hardening

1. Introduction

Strain hardening is a distinctive feature in crystal plasticity, where the flow stress increases during load application due to the development of an entangled dislocation network [1–3]. The physical underpinning between plastic flow and the increase in dislocation density is however absent in submicrometer-sized crystals where dislocation annihilations at the free surface limits dislocation storage [4–6]. In such confining sample sizes, sudden activation and deactivation of surface-truncated (single-ended) dislocation sources under increasing applied stresses produces an intermittent supply of mobile dislocation segments. As such source-exhaustion hardening mechanisms come into play, the stress–strain curve is found to exhibit marked plastic bursts [7–9].

A central aspect in the understanding of crystal plasticity concerns assessment of the transition between confining and bulk plastic flow [10–13]. This is a complex issue to analyze because of the vast dislocation density arising in micrometer-sized samples [13] and its sensitivity to loading orientation. Onset of bulk strain hardening would be therefore facilitated in dislocation networks arising under such multiple-glide loading orientations that exhibit strong dislocation interactions and storage. Surface dislocation annihilations and the emergence of confining plasticity would then be enhanced in multiple or single glide orientations where milder dislocation interactions occur.

The fundamental discreteness of crystal plasticity is due to the onset of dislocation avalanches. Mean-field statistical analyses indicate that the probability density of dislocation avalanche slips fulfills a universal power-law (scale-invariant) form similar to that describing other physical instabilities such as earthquakes in fault systems [14–17]. Knowledge is however unavailable on whether transition from bulk to confining plasticity fundamentally affects avalanche development.

The following are the main purposes for this investigation. First, we seek to provide a thorough analysis to the emergence of strain hardening in small sample dimensions. Mean-field (continuum) crystal plasticity is central to this work, as the behavior of a random dislocation population is averaged using uniform dislocation densities. Whereas a preconceived idea appears to be that such analyses may not hold in microscopic crystals [12,18,19], our experiments show that a deterministic understanding to microscale plasticity and its evolution across sample dimensions

* Corresponding author; e-mail: jorge.alcala@upc.edu

http://dx.doi.org/10.1016/j.actamat.2015.02.027
1359-6462/

becomes accessible through this scheme. Secondly, it is our purpose to furnish experimental evidence on the influence of strain hardening upon the size distribution of dislocation avalanches. This investigation therefore provides a solid mean-field mechanical and statistical comprehension to the evolution of plasticity across sample dimensions.

2. Uniaxial stress–strain curves and the counting of dislocation avalanches

Present investigation comprises 40 micropillar compression experiments performed in copper single crystals with diameters $D = 1.2$, 2.0, 7.0 and 20 μm and aspect ratio (diameter:length) of 1:3. The micropillars were manufactured by Focused Ion Beam (FIB) milling from (i) a well-annealed copper single crystal with the $\langle 1\,1\,1\rangle$ orientation and (ii) single grains with the $\langle 0\,1\,2\rangle$ and $\langle 0\,0\,1\rangle$ orientations – as measured by Electron Back-Scatter Diffraction (EBSD) – from a polycrystalline copper sample. This polycrystalline sample had been previously heat-treated in vacuum to obtain substantial grain growth to a final average size of 30 μm. During machining, FIB energy was set at 30 keV while a low value of 180 pA was selected for the beam current in the final step.

The load–displacement curves were recorded using an in-house system operating in true displacement (strain) control inside the chamber of a Scanning Electron Microscope (SEM). This allows for unique assessments of dislocation avalanches. The imposed displacement rate was set to 2 nm/s in all experiments. Representative uniaxial stress–strain curves are shown in Fig. 1(a) and (b).

Plastic intermittencies produced at an externally applied strain-rate of $\approx 4 \times 10^{-4}\,s^{-1}$ are illustrated in the highly magnified portions of the stress–strain curves in Fig. 2. Uniaxial displacements Δu_i containing a number of stress serrations (where each serration is associated with an individual dislocation avalanche) are shown in Fig. 2(a). One such plastic displacement Δu is characterized in that the applied stress remains below its initial level as marked by the arrows in Fig. 2(a). In the absence of strain-rate effects, this is equivalent to a plastic intermittency produced in more conventional experiments driven under load (stress) control. The associated slip is then given by:

$$s_\sigma = \frac{\Delta u}{\mathrm{SF}} \tag{1}$$

where SF is the Schmid factor in the active slip systems.

Fig. 2(b) shows slip s_ε produced by an individual dislocation avalanche. The avalanche is characterized by stress serration $\Delta\sigma = \sigma_{\max} - \sigma_{\min}$ and by plastic displacement Δu accumulating along the pillar length l. Since $s_\varepsilon \times \mathrm{SF}/l$ is the accumulated uniaxial plastic strain $\Delta\varepsilon$, which necessarily equals $\Delta\sigma/E$, it follows that:

$$s_\varepsilon = Nb = l\Delta\sigma/(E \times \mathrm{SF}), \tag{2}$$

where N is the number of dislocations contained in the avalanche, b is the magnitude of the Burgers vector and E is the elastic stiffness of the compressed micropillar.

Experimental fluctuations during testing translate into an uncertainty of $\Delta\sigma = 1$ MPa. Current statistical analyses of dislocation avalanches are performed with an uncertainty stress threshold $\Delta\sigma$ that is 3 times greater, so that the size of the minimum discernable slip becomes

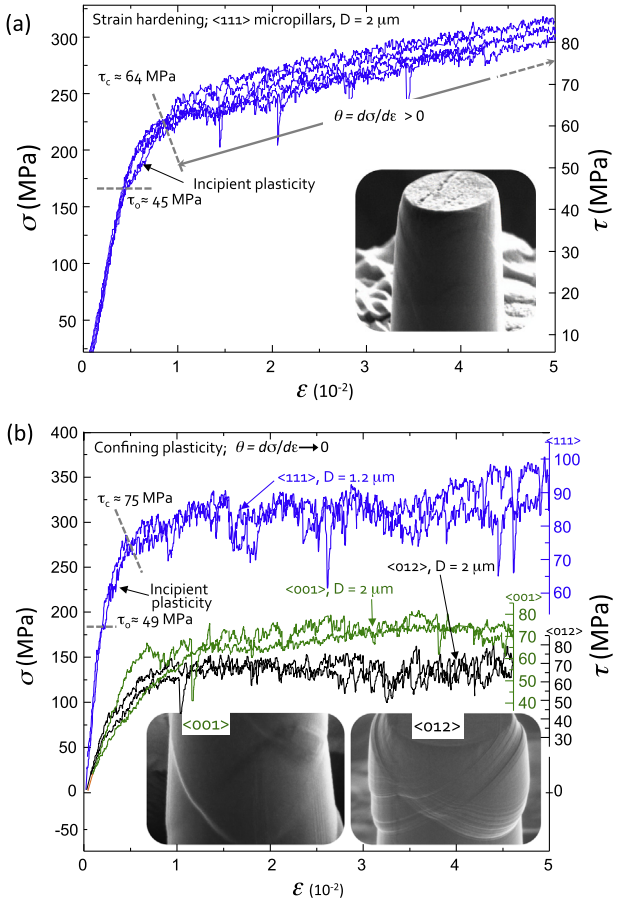

Fig. 1. Uniaxial stress (σ)—logarithmic strain (ε) curves for different micropillar diameters and orientations. (a) $\langle 1\,1\,1\rangle$ micropillars deforming within the strain hardening domain. The inset shows rather continuous flow along the micropillar length with faint slip traces. (b) Confining plasticity where the insets show slip traces including dual glide deformation patterns for $\langle 0\,1\,2\rangle$ micropillars. For all micropillar orientations in the figures, the stage of incipient plasticity attains at intermediate values from τ_o and τ_c.

$s_\varepsilon = 1.86b$, $1.43b$ and $1.84b$ for the $\langle 1\,1\,1\rangle$, $\langle 0\,1\,2\rangle$ and $\langle 0\,0\,1\rangle$ pillar orientations, respectively (Eq. (2)).

3. Theoretical background and mean-field models

3.1. Bulk crystal plasticity and the mean free path traveled by dislocations

Continuum descriptions of crystal plasticity allow prediction of the stress–strain curves in bulk single crystals. Advanced models are based on the detailed knowledge of short-range stresses that govern junction formation [20,21]. Short-range interactions are smoothened in space so that the critical shear stress τ^α for dislocation mobilization in any arbitrary slip system α scales with the forest dislocation density ρ^β (length of dislocation lines per unit volume) in all interacting slip systems β. This is expressed by:

$$\tau^\alpha = \mu b \sqrt{\sum\nolimits_\beta a_{\alpha\beta}\rho^\beta}, \tag{3}$$

where α and β run from 1 to 12 to account for all slip systems in fcc crystals, $a_{\alpha\beta}$ is a matrix prescribing